

THERMOLUMINESCENT RESPONSE OF LiF:Mg TO

GAMMA AND NEUTRON RADIATION

by

NALINI KHANNA

M.Sc., Indian Institute of Technology, N. Delhi, INDIA, 1970

---

A MASTER'S THESIS

submitted in partial fulfillment of the  
requirements for the degree

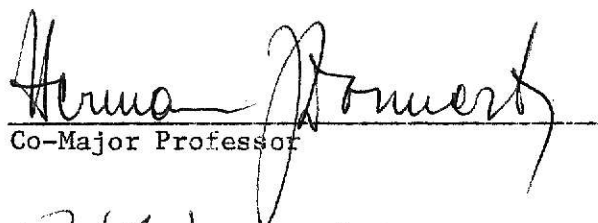
MASTER OF SCIENCE

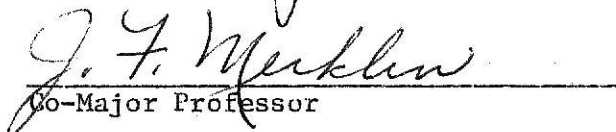
Department of Nuclear Engineering

KANSAS STATE UNIVERSITY  
Manhattan, Kansas

1973

Approved by:

  
Co-Major Professor

  
Co-Major Professor

-D  
2668  
T4  
1973  
K43  
C.2  
Docu-  
ment

## TABLE OF CONTENTS

1.	INTRODUCTION . . . . .	1
2.	THEORY . . . . .	4
2.1.	Explanation of Solid State Terminology . . . . .	4
2.2.	Simple Model of TL . . . . .	9
2.3.	Radiation Dose Response . . . . .	9
2.4.	TL Dosimetry . . . . .	10
2.5.	Randall-Wilkins Theory . . . . .	11
2.6.	Model for Supralinearity . . . . .	12
3.	THERMOLUMINESCENT DOSIMETRY . . . . .	14
3.1.	Thermoluminescent Response of LiF:Mg . . . . .	14
3.2.	Factors Affecting LiF Thermoluminescence . . . . .	14
4.	EXPERIMENTAL . . . . .	22
4.1.	Dosimeters . . . . .	22
4.2.	Reader Unit . . . . .	23
4.3.	Gammacell . . . . .	26
4.4.	Neutron Source . . . . .	31
5.	DETERMINATION OF THE CALIBRATION CURVES . . . . .	34
5.1.	Necessity . . . . .	34
5.2.	Gamma Calibration Curve . . . . .	34
5.3.	Neutron Calibration Curve . . . . .	41
6.	DISCUSSIONS AND CONCLUSIONS . . . . .	47
7.	ACKNOWLEDGEMENTS . . . . .	50
8.	LITERATURE CITED . . . . .	51
9.	APPENDICES . . . . .	54
	Appendix A . . . . .	55
	Appendix B . . . . .	56

## LIST OF FIGURES

2.1.	Energy band model of a crystal . . . . .	5
2.2.	Schematic representation of some important color centers in alkali halides . . . . .	6
2.3.	Trap depth in a crystal . . . . .	7
3.1.	A typical glow curve for TLD-100 . . . . .	15
4.1.	EG and G Model TL-3B thermoluminescent dosimeter reader . . . . .	24
4.2.	Block diagram of the EG and G Model TL-3B reader . . . . .	25
4.3.	A typical chart record obtained from EG and G Model TL-3B reader for the TL-21 dosimeter after partial annealing . . . . .	27
4.4.	EG and G Model TL-81B read head adapter . . . . .	28
4.5.	A view of the Gammacell-220 . . . . .	30
4.6.	Plexiglass $^{252}\text{Cf}$ source holder with source location . . . . .	32
4.7.	A cross-section view of the $^{252}\text{Cf}$ facility . . . . .	33
5.1.	The $^{60}\text{Co}$ gamma calibration curve in the dose range 0-7000 rad for the EG and G Model TL-21 dosimeters . . . . .	38
5.2.	The $^{60}\text{Co}$ gamma calibration curve in the high dose region for the EG and G Model TL-21 dosimeters . . . . .	39
5.3.	The $^{60}\text{Co}$ gamma calibration curve for the EG and G Model TL-21 dosimeters . . . . .	40
5.4.	The $^{252}\text{Cf}$ neutron calibration curve in the fluence range 0 to $7.5 \times 10^{11} \text{ n/cm}^2$ for the EG and G Model TL-21 dosimeter . . . . .	43
5.5.	The $^{252}\text{Cf}$ neutron calibration curve in the high fluence region for the EG and G Model TL-21 dosimeter . . . . .	44
5.6.	The $^{252}\text{Cf}$ neutron calibration curve for the EG and G Model TL-21 dosimeters . . . . .	45

## LIST OF TABLES

3.1.	Effect on Production of F-Centers . . . . .	18
3.2.	Glow curve areas produced from F-center concentration of 2 x 10 <sup>18</sup> cm <sup>-3</sup> . . . . .	19
5.1.	Parameters obtained from analysis of data for the gamma calibration curve . . . . .	37
5.2.	Parameters obtained from analysis of data for the neutron calibration curve . . . . .	46



## 1. INTRODUCTION

Detection and measurement of ionizing radiation have long been important in the physical and life sciences. Soon after the discovery of ionizing radiation, the need for appropriate dosimetry was realized. It was not only the radiation hazard involved in the use of ionizing radiation, but its controlled use in the fields of medicine, biology, industry and research, which necessitated the precise measurement of radiation energy absorbed. This led to considerable interest in this field and over the last decade or two, significant progress has been made.

The determination of radiation dose by measuring the effect of radiation is termed Radiation Dosimetry. Radiation dose is the amount of energy deposited in an absorbing material and is dependent on the type and energy of the radiation.

The basic unit for radiation exposure due to gamma rays is the roentgen defined as "that amount of x- or gamma radiation such that the associated corpuscular emission per 0.001293 g of air produces, in air, ions carrying one electrostatic unit of quantity of electricity of either sign" (1). A more useful unit of radiation dose is the rad, which is equivalent to 100 erg absorbed per gram in the material in which the absorption occurs.

Initially, around the turn of the century, there were no suitable measuring instruments and no definition of units. For nearly forty years, the ionization chamber and photographic emulsions were the only measuring devices in use. During the last 20 years, techniques like "chemical dosimetry" and "solid state dosimetry" were developed. Solid state dosimetry is based on the effects of radiation in solids. Certain types of crystals

store energy when irradiated with ionizing radiation. Upon being heated they release the stored energy in the form of light--this phenomenon is termed thermoluminescence (TL).

Thermoluminescence has been known for centuries (2) and is commonly observed in certain rocks, especially certain fluorites and lime stones, when they are heated. Daniels (3) was the first to propose the application of TL in radiation dosimetry. It was not long after that when the use of Lithium Fluoride (LiF) as a sensitive phosphor was established. Since then numerous investigations (4,5) on the TL characteristics of various phosphors have been reported. Several synthetic phosphors showing a high sensitivity to radiation have also been developed (6,7,8). Some desirable characteristics of phosphors for TL dosimetry are listed by Schulman (9), and Spurny (10).

Thermoluminescent dosimeters (TLD's) have several advantages. They are useful over a wide range of dose ( $10^{-4}$  to  $10^6$  R) and are sensitive to alpha, beta, gamma, neutron and proton irradiation. They are compact, precise, easily read and reusable. The only drawbacks are that they require calibration prior to use in unknown radiation fields, they are sensitive to impurities and therefore are not easily reproducible and the reader equipment is complicated and expensive.

Since the introduction of TL techniques in radiation dosimetry, LiF has received considerable attention. It is available in three forms: TLD-100 (natural LiF) containing 92.5%  $^7\text{Li}$  and 7.5%  $^6\text{Li}$ , TLD-600 containing 95.62%  $^6\text{Li}$  and 4.38%  $^7\text{Li}$  and TLD-700 containing 99.99%  $^7\text{Li}$  and 0.01%  $^6\text{Li}$ . The prominent impurity in all the types is magnesium (Mg). TLD-600 and TLD-700 have been used in thermal neutron and gamma ray mixed field dosimetry (10,11, 12,13). TLD-700 is nearly insensitive to thermal neutrons, responding only

to gamma rays. Above thermal energies, the neutron response of TLD-600 and TLD-700 have been shown to be energy dependent (14). TLD-100 is the most widely used, because of its low cost and commercial availability.

The TLD's used for this study were the externally heated needle dosimeters of LiF and Mg as prominent impurity (LiF:Mg) marketed as TLD-100 by Harshaw Chemical Company, Cleveland, Ohio. The objective of this study was to investigate the response of these dosimeters to different types of radiation namely  $^{60}\text{Co}$  gamma radiation and  $^{252}\text{Cf}$  neutron radiation. The calibration curves for both types of radiations were to be obtained. It was the purpose of this work to study these calibration curves and to investigate the presence of supralinearity. It was also the intent of this work to show the dependence of supralinearity, on the type of radiation.

## 2. THEORY

### 2.1. Explanation of Solid State Terminology

#### 2.1.1. Energy band model of a crystal.

Quantum mechanically the electrons in an isolated atom can exist in stable orbitals around the nucleus for discrete values of energy. Each electron is represented by a wave function  $X_A$  such that  $X_A^2$  measures the density of the charge cloud for this electron. When two atoms A, B are brought together e.g. in a diatomic molecule, the orbitals interact and the resulting molecular orbit is bi-centric instead of mono-centric as in the case of an atom. A suitable physical description could be that each electron moves in an orbit which extends to the neighborhood of both nuclei. The atomic orbital  $X_A$  now becomes the two diatomic orbitals  $X_A \pm X_B$  each with its distinct energy. This process may be extended such that each successive new atom adds one more energy level, at the same time slightly altering those of the previous set. In the crystal the number of atoms is very large  $\sim 10^{23}$  and the resulting  $10^{23}$  energy levels formed are very close together and may be treated as a continuum within a given band. Thus there will be a band associated with each of the allowed orbitals of the original atom.

The structure of a crystal may be then, treated as bands or zones of allowed energies, separated by forbidden zones (Fig. 2.1).

For a complete theory the reader is referred to pertinent literature (15,16).

#### 2.1.2. Traps.

Impurity atoms or lattice irregularities such as vacancies, interstitials, dislocations, or aggregates of one or more of these can give rise

**THIS BOOK  
CONTAINS  
NUMEROUS PAGES  
WITH DIAGRAMS  
THAT ARE CROOKED  
COMPARED TO THE  
REST OF THE  
INFORMATION ON  
THE PAGE.**

**THIS IS AS  
RECEIVED FROM  
CUSTOMER.**

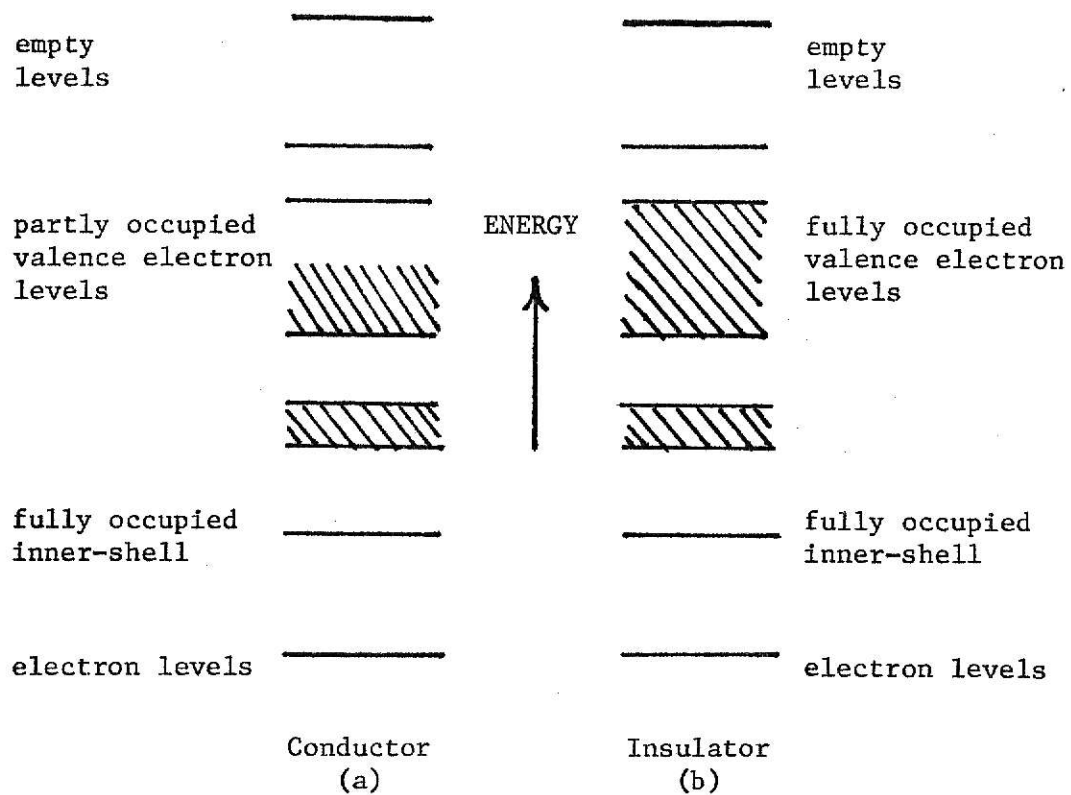
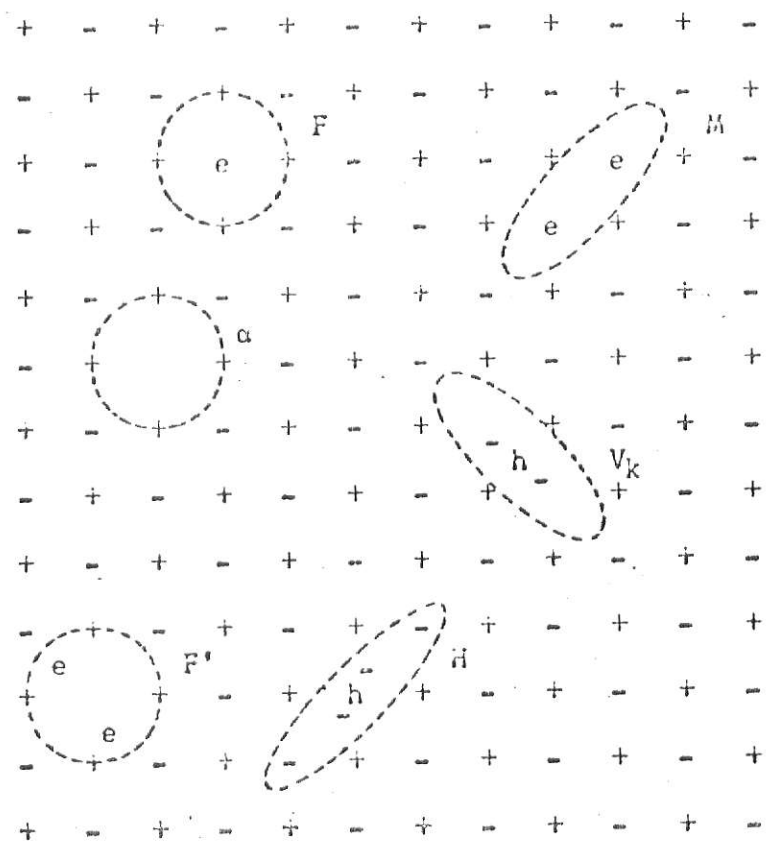


Fig. 2.1. Energy band model of a crystal. The partly filled band in (a) makes the substance a conductor, but the filled bands of (b) make it an insulator.



+ = Alkali ion  
 - = Halogen ion  
 e = Electron  
 h = Hole

Fig. 2.2. Schematic representation of some important color centers in alkali halides.

to localized electron states with narrow energy levels in the forbidden region. These impurity states, capable of capturing an electron or hole are termed traps. The defect centers formed by the trapped charges can have excited states which allow absorption of visible or near ultra violet light, protons. Such defect centers are termed "color centers." Two simple centers are the F-center and the V-center. The F-center is an electron trapped at a negative ion vacancy while the V-center is a hole trapped at a positive ion vacancy. Figure 2.2 shows some important color centers in alkali halides.

### 2.1.3. Trap depth.

For a trapped electron, the trap depth is the energy difference between the trap and the bottom of the conduction band,  $E_1$ , and for a trapped hole, the trap depth is the energy difference between the trap and top of the valence band,  $E_2$  (Fig. 2.3).

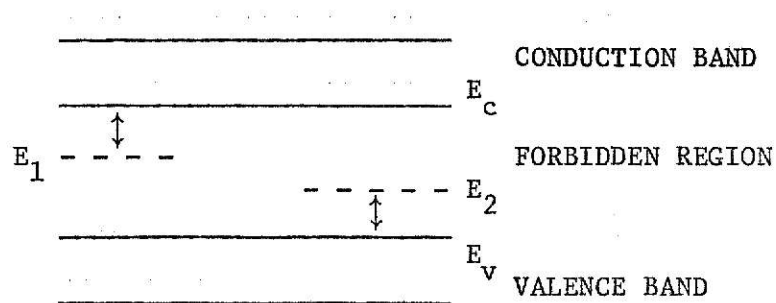


Figure 2.3. Trap depth in a crystal.

### 2.1.4. Luminescence.

Luminescence denotes the emission of energy as visible or near visible radiation. The initial excitation may be by light, particle bombardment,



mechanical strain, chemical reaction or heat. If the transition occurs between states of like multiplicity the phenomenon is termed fluorescence. If the emission arises due to radiative transitions between states of different multiplicity the process is termed phosphorescence (17).

#### 2.1.5. Thermoluminescence.

At room temperature, there is a finite but small probability that traps will give rise to luminescence. As the temperature is raised the probability for release of electrons and holes increases. The phenomenon of accelerating the luminescence by raising the temperature of the crystal is called thermoluminescence.

#### 2.1.6. Phosphor.

A crystal which exhibits luminescence is termed a phosphor. The basis of a phosphor is a pure insulating crystal which is made luminescent by the addition of a small proportion of impurity atoms.

#### 2.1.7. Glow curve.

The energy of the trap depth is directly related to the temperature required to release the electron and produce TL. As an irradiated crystal is heated, the probability of releasing any electron increases. The emitted TL will thus start out weak, go through a maximum and decrease again to zero when all the traps are emptied. A record of the intensity of the emitted light as a function of temperature at a constant heating rate, is known as a TL glow curve. A trap of a given energy depth gives rise to a single glow peak. Most TL phosphors show glow curves made up of a number of glow peaks which may or may not be well resolved.

## 2.2. Simple Model of TL

A unified theory covering all aspects of TL has not so far been formulated but the phenomenon is qualitatively understood.

Radiation produces ionization thereby creating free electrons and holes. These wander in the crystal until they are trapped in metastable states or until they recombine. The metastable states are presumed to be associated with lattice imperfections. If the traps are shallow the electrons may receive enough thermal energy to escape from the trap even at room temperature. This is the case in semiconductors where the energy gap is small and the traps are located slightly below the conduction band. In phosphors however the traps are relatively deep and the electrons have little probability of escape at room temperature. Trap depth therefore is a measure of the suitability of a phosphor for use in TLD. The number of traps filled in an irradiated phosphor is a function of the total dose received. It may also be a function of the dose rate and the quality of radiation. To determine the dose received, the phosphor is heated. As the temperature is raised the probability of the trapped electron being released is increased and the electron is returned to its ground state giving off energy in the form of light photons. An analogous process with holes may also take place, depending upon the relative stability of the electron trap or the hole trap.

## 2.3. Radiation Dose Response

In any radiation dosimetry technique an important characteristic is the response of the system with radiation exposure or dose. Ideally, for reasons of simplicity and convenience of evaluation, a linear dose response curve is desirable. However very few systems respond in this manner.

From the simple model of TL presented earlier, it might be expected that the TL signal obtained would be a linear function of the radiation dose. However, even though the total amount of ionization produced is directly proportional to the radiation dose, the trapping mechanism, the ways in which the trapped electrons or holes are thermally released, the processes by which they recombine to give off light and the nature of traps involved can all influence the final form of the dose response curve. Some phosphors, such as synthetic  $\text{CaF}_2\text{:Mn}$  exhibit a linear dose response over a wide range (18). Others like  $\text{LiF}$  and  $\text{Li}_2\text{B}_4\text{O}_7\text{:Mn}$  show a non-linear response (8). All TL phosphors respond in a linear manner to small amounts of radiation. Also at the other extreme all phosphors show saturation effects and eventually "damage." At saturation, all available traps are filled and hence no more TL results from a further increase of dose. As the dose is increased still further, the entities responsible for the trapping mechanism may be dissociated or disrupted to the extent that they are no longer useful as traps. This can then result in a decrease in the TL, from the saturation level. This usually occurs in the mega-rad region.

#### 2.4. TL Dosimetry

The ionization produced in a material is directly proportional to the amount of radiation absorbed. To a first approximation, the total number of electrons trapped in the metastable states of the crystals in a TL phosphor can be assumed to be a function of the number made available by the irradiation. The released TL is proportional to the number of trapped electrons. Hence a measure of this light can be related to the radiation dose. This is the basis of TLD.

Generally, the integrated light output i.e. the area under a TL versus time glow curve, is used as a measure of the radiation dose. For any one trap the glow peak height can also be used if one uses a reproducible heating rate. In this study the latter technique is employed.

## 2.5. Randall-Wilkins Theory

The theory of TL glow curves has been studied extensively (19,20,21). A simple first order kinetics model was proposed by Randall and Wilkins (20). They assumed that the TL from a given glow peak occurs when a trapped electron is thermally released and returns either to a recombination center or to the ground state. The rate determining process for the luminescence is the rate of escape of the electron from the trap. Each trap has a characteristic trap depth energy "E" and frequency factor "s." The probability per unit time, of release of a trapped electron is

$$p = s \exp(-E/kT)$$

where T is the absolute temperature of the crystal and where k is the Boltzmann constant.

The TL intensity is determined by the rate of emptying of electrons from traps,

$$I = -dn/dt$$

where n is the number of electrons in the traps at time t.

Then,

$$I = -dn/dt = np = ns \exp(-E/kt)$$

If the phosphor is heated at a constant rate,

$$q = dT/dt$$

then  $-dn/dt = -q \, dn/dT = ns \exp(-E/kT)$

$$n_T = n_0 \exp \int_{T_0}^T -s/q \exp(-E/kT) \, dt$$

and 
$$I_T = n_0 [s \exp(-E/kT)] [\exp \int_{T_0}^T -s/q \exp(-E/kT) \, dT]$$

This equation gives a complete description of the glow curve from a single trap. The initial exponential rise of the glow curve is governed by the term in the first brackets. The rapid fall off is due to terms in the second brackets. For a single glow peak it is possible to extract information about the trap depth and the frequency factor from the glow curve. However, for a glow curve with multiple peaks this becomes difficult. Instead, the same information can be obtained by studying the post-irradiation isothermal annealing of the particular glow peak at two or more different temperatures (22).

## 2.6. Model for Supralinearity

Previous models (19,24) for explaining the supralinear response of LiF (TLD-100) postulated the "creation" of additional traps or recombination centers. Mathematical formulations developed using these assumptions gave good agreement with most of the experimental data. However certain features of the experimental observations seemed unreasonable. On the basis of the previous models, the created traps and recombination centers were identical to those initially present. This seems an unlikely coincidence.

Cameron et al (23) proposed a model to account for all experimental observations. The new model assumes the presence of a competing deep trap

with a larger cross-section for the capture of electrons than the normal TL traps. It is also assumed that the total number of these deep traps is much smaller than the number of normal TL traps. Because of the larger cross-section of the competing trap, it has a greater probability of capturing the electrons or holes. As the dose increases, more electron-hole pairs are created and this results in a higher probability of filling both the normal TL traps as well as filling the deep trap. When the LET of the dose is increased further, there is a larger number of electron-hole pairs available in the neighborhood of the traps, and the probability or efficiency of filling either type of trap becomes about equal. When this happens the filling of the competing trap has very little influence on the TL response and this results in a linear response with dose. The reason for assuming the competing trap to be a deep trap lies in the fact that this trap remains filled even after an annealing of 1 hour at 280°C but is emptied after 1 hour at 400°C.

### 3. THERMOLUMINESCENT DOSIMETRY

#### 3.1. Thermoluminescent Response of LiF:Mg

Five peaks appear in the glow curve from LiF. A typical glow curve for LiF:Mg (TLD-100) is shown in Fig. 3.1. It shows the existence of five peaks, appearing at temperatures ranging from about 80°C to 210°C. Each peak corresponds to a particular trap, the energy of the trap depth determining the temperature at which the peak appears. It has been found that peaks corresponding to low temperatures quickly decay even at room temperature. The approximate half-lives of the peaks 1 through 5 are found to be 5 min, 10 hr, 1/2 yr, 7 yr and 80 yr respectively. Peaks 2 and 5 are the most prominent, occurring at temperatures of 105°C and 190°C. Peak 5 is the largest and most stable peak and is generally used for dosimetry purposes.

A characteristic of dosimeter grade LiF is its linear response for exposures up to about  $10^3$  R (23,24,25). Above this, the TL response increases faster with increasing dose, until about  $10^5$  R at which point saturation begins. The behavior in the range  $10^3$  R- $10^5$  R is termed non-linear or supralinear. A suitable explanation of this phenomenon is given in Section 2.6.

#### 3.2. Factors Affecting LiF Thermoluminescence

##### 3.2.1. Preirradiation annealing.

Following irradiation and readout, it is necessary to anneal LiF, as the readout mechanism does not empty all the traps. As shown by Zimmerman et al, the method of annealing has marked effect on the subsequent response

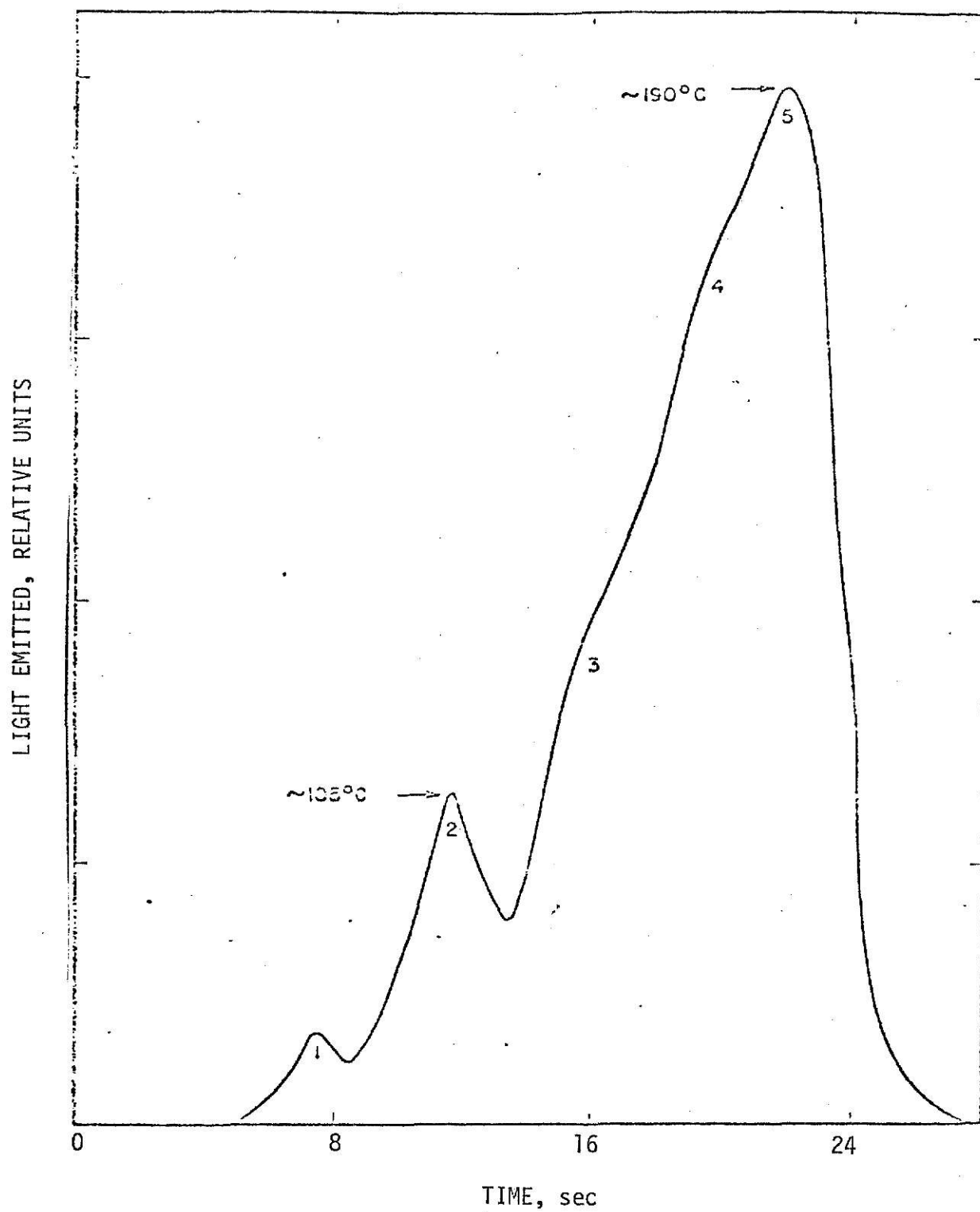


Fig. 3.1. A typical glow curve of TLD-100 after annealing 1 hr at 400°C and irradiation to 100 R (reproduced from Ref. 41).



of LiF. For consistency, it is therefore necessary to adopt and adhere to a suitable annealing procedure.

For the TL-21 dosimeters used in this research (see Section 4.1 for description), a primary annealing at 350°C or 400°C for one hour followed by a 24-hour annealing at 80°C is suggested (36). Zimmerman et al (22) reported that annealing at 400°C for 1 hr removes all effects of any previous annealing, and annealing at 400°C beyond 1 hr has little effect on the glow curve. They also recommended a 80°C annealing for 24 hrs following the 400°C annealing to reduce peaks 1 and 2 relative to the higher temperature peaks.

Kaiseruddin (25) investigated the effect of eliminating the 24 hr 80°C annealing and reported no significant change in standard deviation of the response values. Therefore, he adopted the 400°C annealing procedure for TLD-100. The same procedure of annealing was adopted for this study too.

### 3.2.2. Post irradiation annealing.

To function as a satisfactory dosimeter, a phosphor should have a TL response that is independent of the storage time prior to readout. Endres (12) studied the fading effects in LiF and reported a 5% decrease in the total light output over a period of 15 days. Karzmark et al (26) reported a 10% to 20% decrease in total light output over a period of 3 weeks followed by an increase toward the initial value in 6 to 8 weeks. This fading effect is probably due to the thermal release of lower temperature traps at room temperature. This release leads to two effects.

- 1) a reduction in the total light output due to reduction in height of lower-temperature peaks.

- 2) an increase in the height of high temperature peaks caused by a fraction of the electrons released from low temperature traps falling in the high temperature traps.

Therefore, for consistent results, it is necessary to remove these lower temperatures peaks by a standardized procedure.

Cameron et al (19) reported that low temperature peaks could be removed by post irradiation annealing at 100°C for 10 min. Dean and Larkins (27) reported annealing the dosimeters at 110°C for 7 min. This latter technique was investigated by Kaiseruddin (25). He reported smaller fluctuations in response, and smaller values of standard deviation, after the dosimeters had been subjected to partial annealing. The same procedure was adopted in this study also.

Wilson et al (28) reported that if LiF (TLD-100) was exposed to about 100 kR and then annealed at 280°C for 1/2 hr, the TL response to subsequent exposures was enhanced by a factor of six over its initial TL response to the same exposure. However, annealing at 400°C for 1 hr removed this enhancement. This phenomenon is termed sensitization. Sensitization then consists of exposing the samples to a high dose and then annealing them at 280°C. Materials that are sensitized show an initially high response up to the saturation doses. Near saturation the sensitized and unsensitized samples have nearly the same response.

### 3.2.3. Effect of irradiation temperature.

DeWerd and Cameron (29) performed irradiations of LiF (TLD-100) at 290°C and -54°C. They reported that the response curves obtained at these temperatures were different than that at room temperature. At 290°C, the curve for  $s/s_0$  versus previous exposure, where "s" is increased sensitivity

and " $s_0$ " is initial sensitivity, was more supralinear than that for room temperature irradiation. For the low temperature irradiation, the slope of the curve was twice the slope of the curve at room temperature. In this study all irradiations were carried out at room temperature.

#### 3.2.4. Quality of radiation.

The type of radiation has marked effect on the creation of traps in LiF. Such effects must be well known before a dosimeter is used in an unknown radiation field.

The energy required to produce an F-center in LiF by different types of radiation has been determined by Morehead and Daniels (30) and is reported below.

Table 3.1. Energy (eV) required to produce an F-center in LiF (30).

Radiation	Initial	after $10^6$ R	after $10^8$ R
2 MeV alpha particles	700	700	700
2 MeV electrons	140	140	700
1 MeV gamma photons	62	160	700
Thermal neutrons	65	100	700

Morehead and Daniels (30) also determined the effect of different types of radiation on the glow curve areas for a given F-center concentration created by that radiation. The results are reported in Table 3.2.

Naylor (31) was the first to report that the increased sensitivity leading to the supralinearity is quality dependent. It was suggested by

Wagner and Cameron (32) that in the supralinear and saturation regions, the TL response is related in an inverse manner to the linear ion density or the number of ion pairs formed per micron, in the material, for the radiation used. Suntharlingam (33) tested this hypothesis further by exposing LiF (TLD-100) to radiations with different specific ionization or linear energy transfer (LET). The LET of a charged particle in a medium is defined as  $dE/dl$  where  $dE$  is the average energy locally imparted to the medium by the charged particle in traversing a distance  $dl$ . This definition implies a macroscopic average even though the loss of the kinetic energy of the charged particle is discontinuous. Suntharlingam (33) concluded that there are four different quality dependent effects in the TL response of LiF

- 1) the usual low energy increase in photoelectric cross-section
- 2) the decrease in supralinearity with increase in LET
- 3) the decrease in the response of sensitized phosphor with increase in LET
- 4) the increase in efficiency at low doses with increase in LET

Table 3.2. Glow curve areas produced from F-center concentration of  $2 \times 10^{18} \text{ cm}^{-3}$  (30).

Radiation producing $2 \times 10^{18}$ F-centers $\text{cm}^{-3}$	Area ( $\text{in}^2/\text{mg}$ ) LiF
$10^6$ rad thermal neutrons	2500
$10^6$ rad betatron	2200
$1.5 \times 10^6$ rad gamma photon	2000
$10^7$ rad alpha particles	4000

### 3.2.5. Dose rate.

It is quite reasonable to expect that the response of the dosimeters would depend upon the total dose absorbed. However, it is not apparent that the response would be dependent on the dose rate. Kaiseruddin (25) investigated the response of TL-21 LiF:Mg dosimeters to very high dose rates. His results indicated that the response of the dosimeters was an increasing function of the dose rate. Also the dose rate dependence was itself an increasing function of the total dose given to the dosimeter. This suggested that the kinetic order of the processes involved in the irradiation of the LiF phosphor is different from unity.

### 3.2.6. Lithium isotopic abundance.

As described earlier LiF is available in three different forms:

Phosphor	% $^7\text{Li}$	% $^6\text{Li}$
TLD-100	92.50	7.50
TLD-600	95.62	4.38
TLD-700	99.99	0.01

#### a) Effect on Photon Response

Bliss (34) investigated the response of TLD-600 and TLD-700 to  $^{60}\text{Co}$  gamma rays and reported that the response of TLD-600 was about 20% higher. This might have been due to slight differences in the amount of phosphor in the ampule. Elsewhere in literature (11,35) the responses of both  $^6\text{Li}$  and  $^7\text{Li}$  have been reported to be identical.

#### b) Effect on Neutron Response.

The TL response in LiF due to neutrons is a secondary process resulting from ionizing radiations produced by neutron reactions on Li and F. Since

the cross sections for neutron reactions are energy dependent, it is necessary to consider the neutron response over different energy ranges.

#### 1. Thermal Neutrons.

The response of LiF to thermal neutrons has been investigated by a number of workers (35,43). The  ${}^6\text{Li}(n,\alpha){}^3\text{H}$  reaction has a large (945b) cross section. The 2.06 MeV alpha particle and the 2.74 MeV triton create more traps in the LiF phosphor. Thus  ${}^6\text{LiF}$  has a greater response than  ${}^7\text{LiF}$ . It is assumed that the response of  ${}^7\text{Li}$  to thermal neutrons is negligible, and use of this has been made by using  ${}^7\text{LiF}$  to study the response in a mixed radiation field.

#### 2. Fast Neutrons.

The response of  ${}^7\text{LiF}$  to neutrons is negligible as compared to that of  ${}^6\text{LiF}$  up to about 1.2 MeV in energy (35). Bliss (34) investigated the response of TLD-600 and TLD-700 to 14.7 MeV neutrons and reported that the response of  ${}^7\text{LiF}$  TLD's was lower by about 20% than that of  ${}^6\text{LiF}$  TLD's. In this study irradiations were done with neutrons of energy 2-8 MeV. It is expected that the  ${}^7\text{Li}$  present in TLD-100 would also contribute to the TL response of the dosimeters.

#### 4. EXPERIMENTAL

##### 4.1. Dosimeters

EG and G Model TL-21, "LiF Miniature Dosimeters" were used in this study. The dosimeters consist of about 10 mg of LiF phosphor, vacuum sealed in a glass capillary. The size of the dosimeters is 1.4 mm in diameter and 12 mm in length. The Model TL-21 uses natural LiF, containing 7.42%  $^6\text{Li}$  and 92.58%  $^7\text{Li}$ , with addition of Magnesium, Aluminum and Titanium (24), obtained from Harshaw Chemical Company as TLD-100 brand. Previous investigations (24) indicate that Magnesium is the major impurity present, hence the phosphor is referred to as LiF:Mg.

When combined with the high detectability obtainable with the Model TL-3B reader, a dose as low as 10 mR can be measured with a precision of  $\pm 2$  mR (36). The dosimeter exhibits the characteristic nonlinearity of LiF at doses above  $10^3$  R and is useful to  $10^5$  R (36). Response in the higher dose range was reproducible but non-linear. To use the dosimeters in the higher dose range pre-calibration was required. The response was dependent upon the energy of the radiation, but independent of slight temperature changes.

Reproducibility of the dosimeters was  $\pm 3\%$  above a dose of 1 R and  $\pm 20\%$  at a dose of 10 mR. Due to small fluctuations in the weight of the phosphor, grain size, geometry of ampule and phosphor sensitivity, the response of the dosimeters from a batch selected by the manufacturers was supposed to be within  $\pm 10\%$  of the mean.

#### 4.2. Reader Unit

An EG and G Model TL-3B Thermoluminescent Dosimeter Reader was used to read the dosimeters. The function of this unit was to heat the dosimeters providing a reproducible constant heating rate, detect the light emitted by means of a photomultiplier (PM) tube, convert the emitted light to an electrical signal, and provide a chart record of the glow curve. The unit was enclosed in a single aluminum cabinet 18 inches x 20 inches x 13 inches. The reader unit is shown in Figure 4.1.

A block diagram of the reader unit circuitry is shown in Fig. 4.2. A regulated current supply fed the read head adapter (described later) in which the dosimeter was positioned. When the READ push button was depressed, a heater current of 6.5 A was supplied to the read head. Light emitted from the dosimeter was reflected toward the PM tube. The signal from the PM tube was routed through the automatic ranging circuit to the pen servo-mechanism. Initially the PM tube was set to its maximum sensitivity, which gave the lowest range on the recorder. When the output increased beyond this range the sensitivity of the PM tube was lowered by a factor of 10 by the automatic ranging circuit. The control logic sequenced these events so that readings from the lowest full scale range, 50 mR to the highest full scale range, 5 kR were possible with a single operation of the READ button. Upon completion of the readout, the status indicator gave the full scale range of the recorder.

A reference signal was provided which enabled the system to be adjusted for accurate readings relative to a known reference. The reference source contained  $^{14}\text{C}$  mixed with thermoluminescent Calcium Fluoride, and was





Fig. 4.1. EG and G Model TL-3B Thermoluminescent Dosimeter Reader.

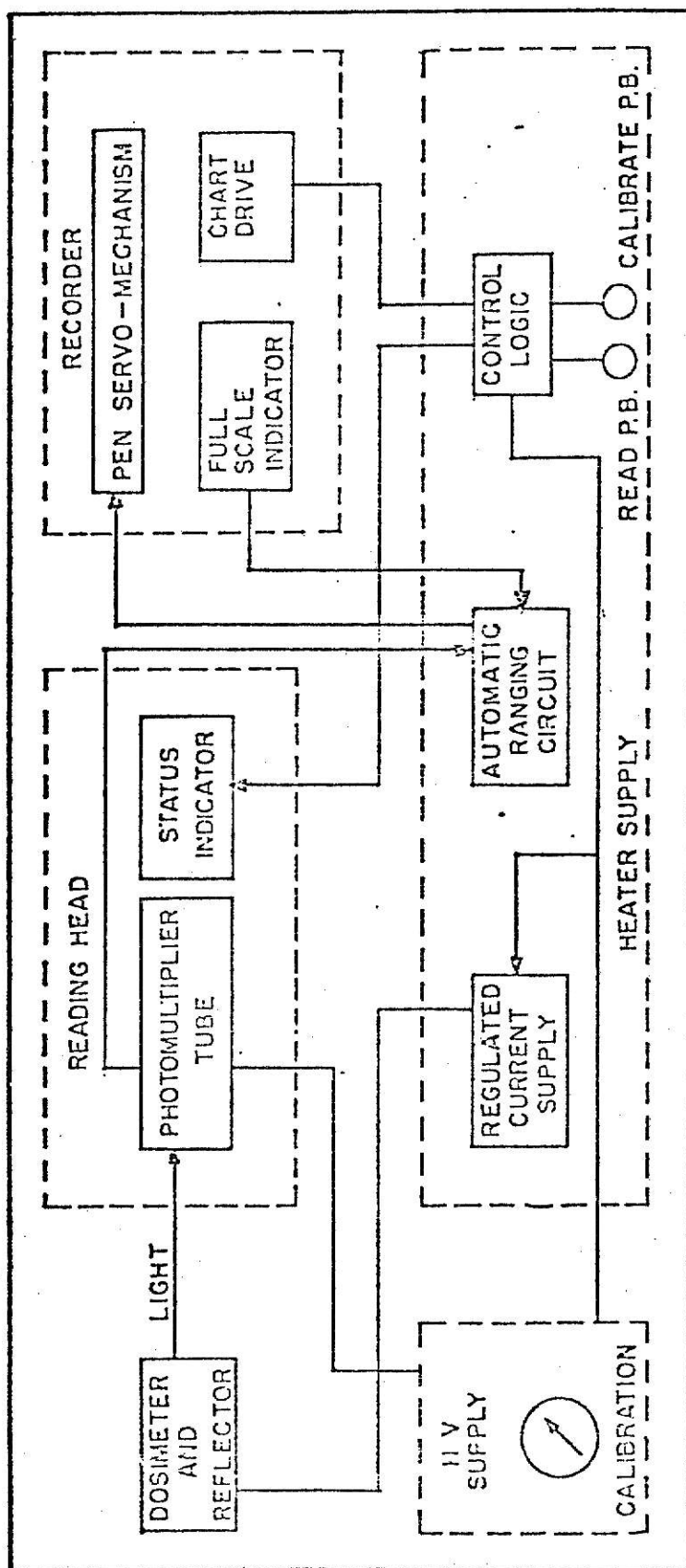


FIG. 4.2. A BLOCK DIAGRAM OF THE EG AND G MODEL TL-3B READER

constructed for use with the Model TL-81 read head adapter. The light output from the standard C-14 source was equivalent to 340 mR with a TL-32A reference dosimeter. The calibration was accomplished by changing the high voltage across the PM tube. The normal working range of the reader was 5 mR to 5 kR with the standard dosimeter, but it could be extended down to 0.5 mR or up to 50 kR by respectively increasing or decreasing the gain of the PM tube.

A typical chart record obtained on this reader with TL-21 dosimeters is reproduced in Fig. 4.3. The heater current turned on when the pen reached the short vertical line near the center of the chart and turned off at the end of the chart. Each time a change of scale took place, the pen produced a vertical "pip." Thus, the final range could be ascertained by counting the number of "pips" as well as by reading the status indicator.

The EG and G Model TL-81B read head adapter shown in Fig. 4.4 was used in conjunction with the reader unit to position and heat the dosimeters. The read head adapter was inserted in the front of the reader unit and enclosed the dosimeter in a light tight chamber. The adapter consisted of a heating coil and a shunt resistance which could be adjusted to regulate the current such that the primary peak occurred in the middle of the three lines on the left side of the chart (see Fig. 4.3).

Since the heating cycle was reproducible for each dosimeter, the peak height could be used as a measure of TL, rather than the entire area under the glow curve.

#### 4.3. Gammacell

A Gammacell-220 unit manufactured by Atomic Energy of Canada Ltd. was used to irradiate the dosimeters. The Gammacell was loaded with a 3,963 Ci

# **ILLEGIBLE DOCUMENT**

**THE FOLLOWING  
DOCUMENT(S) IS OF  
POOR LEGIBILITY IN  
THE ORIGINAL**

**THIS IS THE BEST  
COPY AVAILABLE**

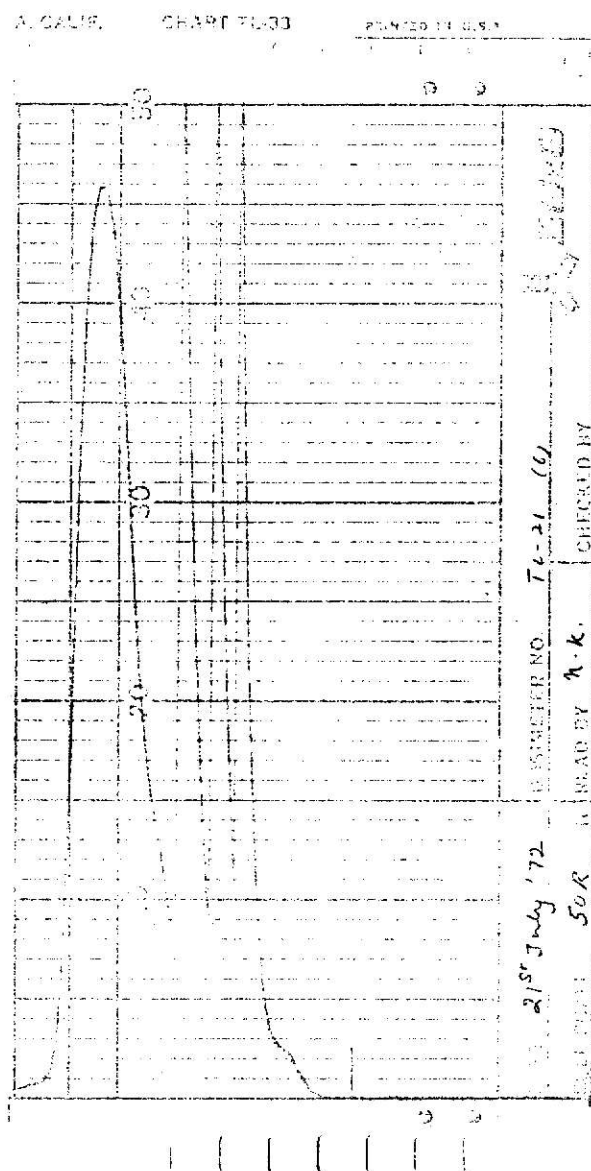


Fig. 4.3. A typical chart record of the EG and G Model TL-21 dosimeters after partial annealing.

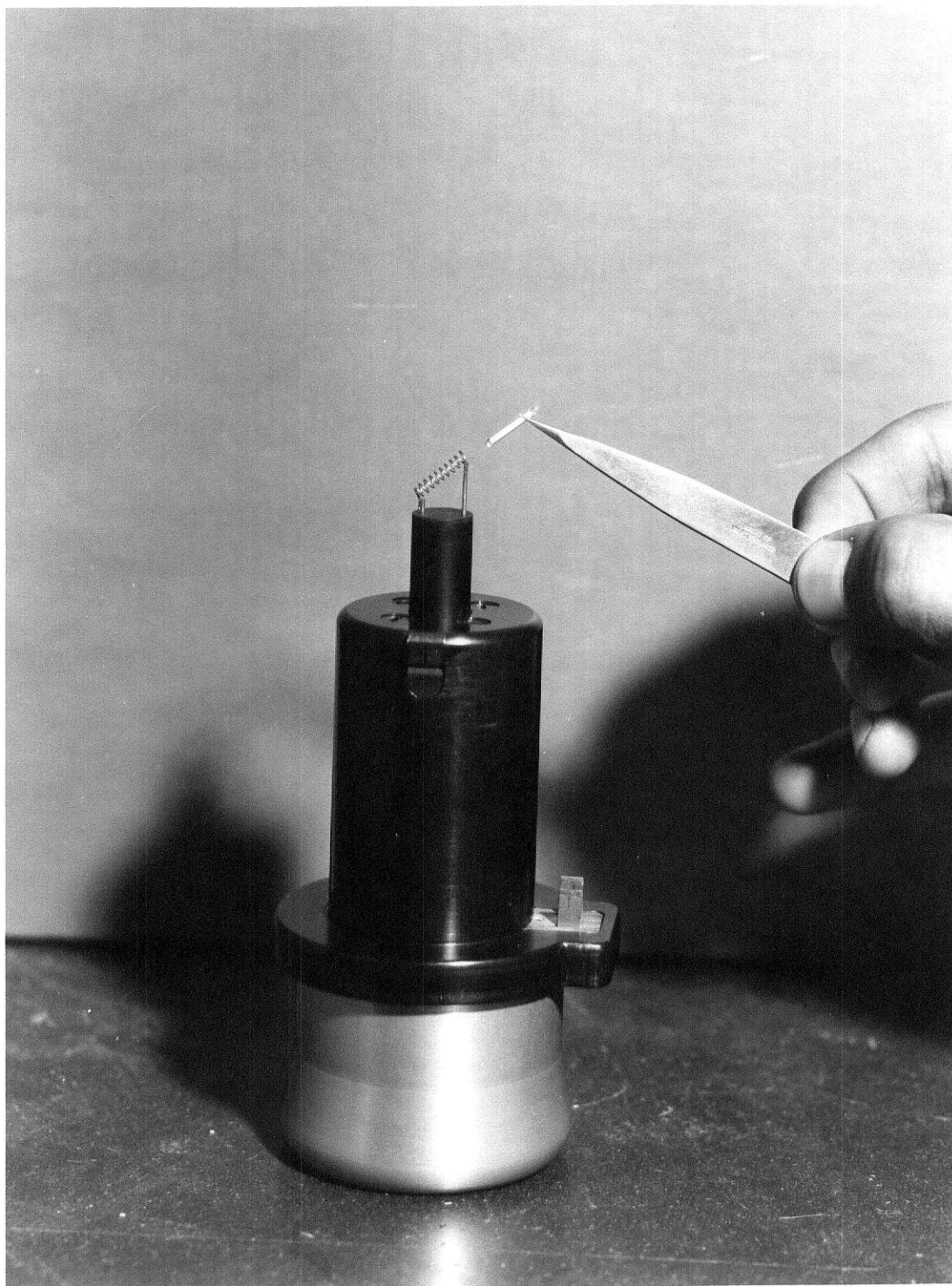


Fig. 4.4. EG and G Model TL-81 B Read Head Adapter.

$^{60}\text{Co}$  source on March 15, 1965. The  $^{60}\text{Co}$  source consisted of 12 linear source elements equally spaced in a stainless steel rack to form a radioactive cylindrical shell. Each linear element consisted of a welded stainless steel pencil filled with metallic cobalt. The internal dimensions of each pencil were 0.395 inch in diameter and 8 inch in length.

A motor driven drawer of the assembly consisted of a steel-encased lead cylinder 53.75 inch long and 6.5 inch in diameter. The drawer was centrally located in a surrounding radiation shield and was driven vertically through the center of the source. The drawer consisted of solid upper and lower sections with a hollow sample chamber. The material to be irradiated was placed in the sample chamber which could be lowered to the center of the source. The sample chamber was 8 inch high and 6 inch in diameter.

The Gammacell was controlled from a panel at the side of the unit. The control panel included a drawer "UP" button, a drawer "DOWN" button, a digital timer with a range of 0 to 999 hours and a timer "IN" switch which enabled the timer to be admitted into the control circuit when desired.

Correct dose rate at the time of irradiation was obtained from a chart associated with the Gammacell.

A polyethylene disc about 1/2 inch thick made to fit inside the irradiation chamber of the Gammacell, was used to irradiate the dosimeters. The dosimeters were inserted vertically in the disc along the circumference of a circle 2 inch in diameter. The circle was concentric with the center diameter of the disc. This insured that all dosimeters irradiated at the same time received the same amount of dose. The disc provided a consistent positioning and holding device for uniformity of all irradiations. All the dosimeters received the same dose by virtue of being placed on an isodose.





Fig. 4.5. A View of the Gammacell-220



The isodose curve as supplied by the manufacturer was 2.75 inch above the base of the chamber and two inch from the axis, in order to receive the dose equivalent to the dose at the center of the chamber. Polyethylene was used due to its small absorption property for *gamma*-rays. The Gammacell with dosimeter holder in place is shown in Fig. 4.5.

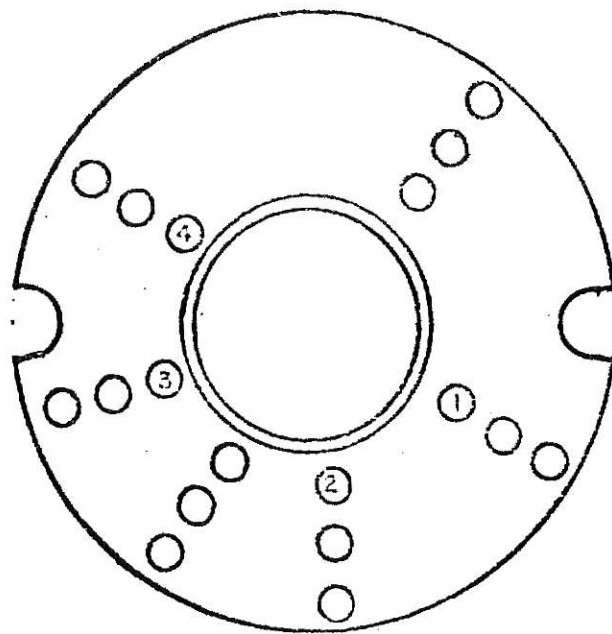
#### 4.4. Neutron Source

A  $^{252}\text{Cf}$  source supplied by Savannah River Laboratory was used as a neutron source to irradiate the dosimeters.  $^{252}\text{Cf}$  has an effective half-life of 2.646 years and continuously emits neutrons with a fission spectrum.

The  $^{252}\text{Cf}$  source with a total weight of 40.86 mg was in the form of four SR-CF-100 series capsules. Figure 4.6 shows the position of these capsules. The source was loaded in April 1971 and was located at the bottom of a thick water shield. A central thimble of 1.65 inch in diameter was located in the middle of the source.

The neutron flux in the central thimble near the sources was measured to be  $6.0 \times 10^9 \text{ n/cm}^2 \text{ sec}$  in July 1972 (37).

The dosimeters were placed on the circumference of a polyethylene disc, about 1/2 inch thick and 1 inch in diameter. This dosimeter holder fits the bottom of a polyethylene capsule which was used to hold the samples as they travelled to and from the control thimble. The four  $^{252}\text{Cf}$  capsules were in the configuration shown in Fig. 4.6. The capsule was made to travel up and down the control thimble by means of a pulley arrangement. The capsule could be ejected by remote control. The travel time was around 10 sec which was much smaller than the total time of irradiation, also it was not constant of every irradiation depending upon personal error. Hence the dose incurred during that time was neglected in this study.

LEGEND

- |   |                            |
|---|----------------------------|
| ① | 8.4 mg                     |
| ② | 10.5 mg                    |
| ③ | 11.1 mg                    |
| ④ | 10.8 mg                    |
| ○ | POSSIBLE POS<br>FOR SOURCE |

FIG.4.6. PLEXIGLASS  $^{252}\text{Cf}$  SOURCE  
HOLDER WITH SOURCE LOC-  
ATIONS.

**ILLEGIBLE**

**THE FOLLOWING  
DOCUMENT (S) IS  
ILLEGIBLE DUE  
TO THE  
PRINTING ON  
THE ORIGINAL  
BEING CUT OFF**

**ILLEGIBLE**

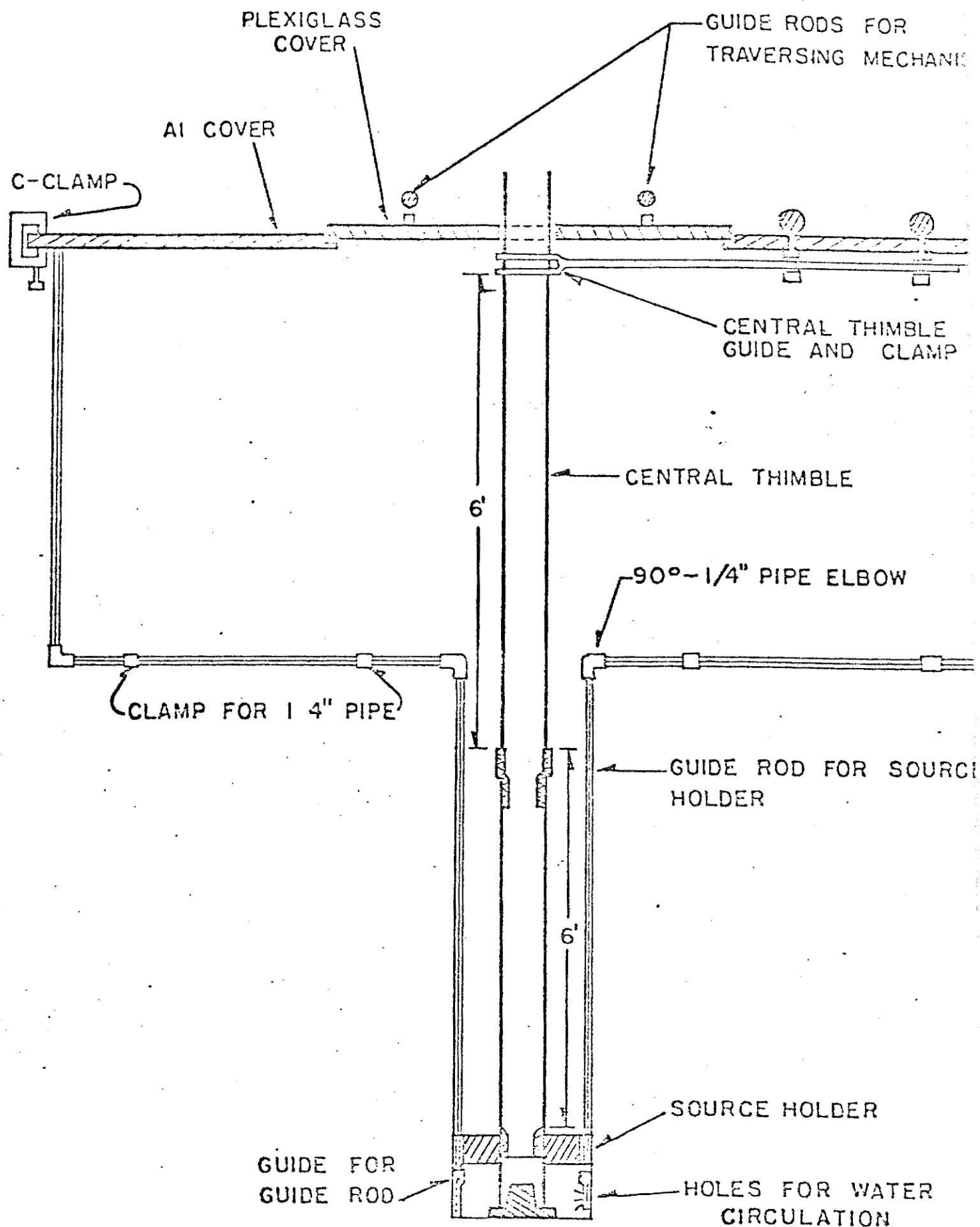


FIG.4.7. A CROSS SECTION VIEW OF THE 252Cf FACILITY.

## 5. DETERMINATION OF THE CALIBRATION CURVES

### 5.1. Necessity

Since the peak height measured on the glow curve from the EG and G reader unit gave the dosimeter response in relative units, it was necessary to obtain a calibration for converting response to dose or response to neutron fluence. Over the range 0 to  $10^3$  rad the response was supposed to be linear with respect to dose. Therefore, a calibration factor could be obtained for use over this range. In the range  $10^3$  to  $10^5$  rad, the response was supposed to be reproducible but non-linear with respect to dose. Thus, a full experimental calibration curve was required over this range.

### 5.2. Gamma-Ray Calibration Curve

#### 5.2.1. General considerations.

The dose rate in the Gammacell at the time of the experiment was 33.25 rad/sec. This was obtained from a chart associated with the Gammacell. The timer equipped with the Gammacell allowed irradiation for any length of preset time. However, the timer did not start counting until the drawer of the assembly was in its lowest position. Therefore, the dosimeters received a dose during the pre-set time as well as some dose while the plunger was traversing up and down. Since the traverse time is a constant, the dosimeters receive a constant dose,  $D_o$ , each time in addition to the dose received during irradiation in the preset time.

In order to determine the additional dose,  $D_o$ , the following mathematical model was used. If the dose rate in response units was represented by  $\dot{R}$ , the response due to the constant additional dose by  $R_o$ , and the pre-set

irradiation time by  $t$ , then the total response of the dosimeters,  $R$ , is given by

$$R = R_0 + \dot{R}t \quad (5.1)$$

The parameters  $R_0$  and  $\dot{R}$  could be obtained by a least-squares analysis of the experimental response values in the range 0 to  $10^3$  rad. Over the linear range, the calibration factor (cf), having units of rad per reader unit could then be obtained by dividing the known dose rate,  $\dot{D}$ , by the dose rate in reader units,  $\dot{R}$ . The dose absorbed during the travel time is then the product of (cf) and  $R_0$ . The total dose was then given by

$$D = D_0 + \dot{D}t \quad (5.2)$$

#### 5.2.2. Experimental procedure.

The dosimeters were annealed for 1 hour at  $400^\circ\text{C}$  before irradiation and then subjected to partial annealing at  $110^\circ\text{C}$  for 7 min following irradiation. They were allowed to cool to room temperature before being read. Groups of eight dosimeters were exposed to doses ranging from 200 rad to 2800 rad. Higher exposures were not used as this might have caused permanent damage in the phosphor thereby rendering them useless for further work.

#### 5.2.3. Analysis of data and results.

Eight response values were available for analysis for each experimental point. The mean response and the standard deviation of the response at each point was calculated.

The first five points were used in the linear regression for estimating  $R_0$  and  $\dot{R}$ . The values obtained from the above analysis were  $R_0 = 13.228$  (reader unit) and  $\dot{R} = 3.765$  (reader unit/sec). The calibration factor was

then obtained as 8.83 (rad/reader unit) and  $D_0$  was obtained by the product of (cf) and  $R_0$  as 116.804 rad. The total dose  $D$  was then obtained by equation (5.2). These values are presented in Appendix A.

Figure 5.1 is the response curve in the range 0 to 7000 rad plotted on linear scales. This indicates clearly that the response is linear in both the low dose and the high dose region, but that the slope in the high dose region is greater than that in the low dose region. Figure 5.2 is the response curve over the complete range from 0 to 30,000 rad showing the points in the high dose region.

Figure 5.3 is the calibration curve obtained by plotting the total dose as the abscissa and the TL response as the ordinate on logarithmic scales. The curve was linear over the range 0 to  $10^3$  rad. Above that, the slope was greater, implying that the TL response increases faster with increasing dose. The curve was divided into two dose regions, the low dose region (0-1113.0 rad) and the high dose region (1113.0-27381 rad). In each region, the data were fitted to a linear model using a weighted least square analysis. The results are presented in Table 5.1.

The linear equations obtained for the two regions were

$$R_1 \text{ (R.U.)} = (0.1165 \text{ R.U. rad}^{-1}) D - 1.0010 \text{ (R.U.)} \text{---low dose region}$$

$$R_2 \text{ (R.U.)} = (0.3076 \text{ R.U. rad}^{-1}) D - 432.0190 \text{ (R.U.)} \text{---high dose region}$$

The two lines in Fig. 5.3 are plots of the above equations. The ratio of the slopes of  $R_2$  to  $R_1$  is 2.64 indicating that supralinearity is present. The break point at which this effect starts is between 1113 and 2111 rad (corresponding to 127 R.U. and 262 R.U.).

TABLE 5.1

Parameters obtained from analysis of data for the  
gamma calibration curve.

Low Dose Region	Slope (R.U./rad)	Y-intercept (R.U.)
Low Dose Region	$0.1165 \pm 0.0073$	$-1.00.0 \pm 6.5859$
High Dose Region	$0.3076 \pm 0.0218$	$-432.0190 \pm 86.3697$



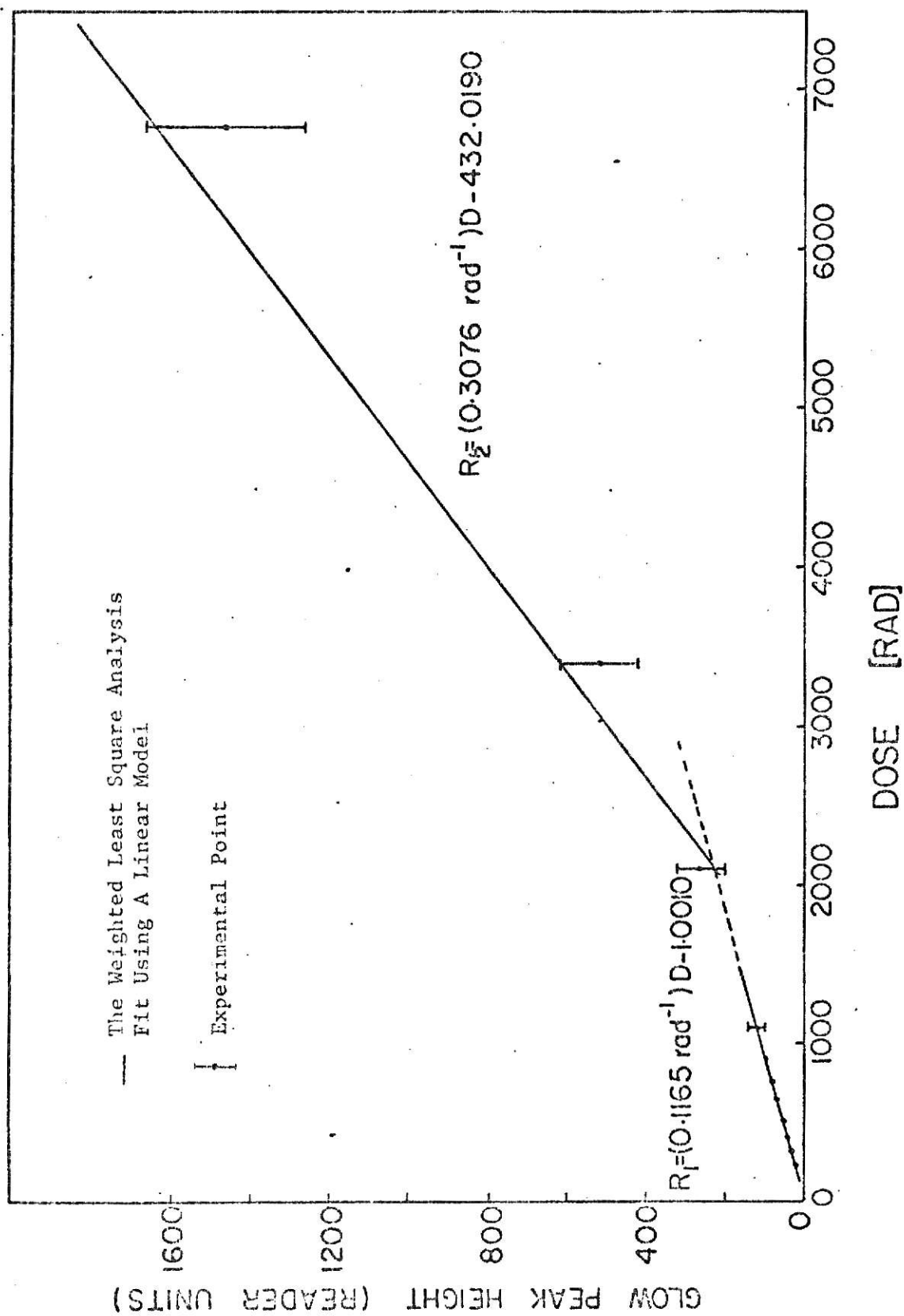


Fig. 5.1. The  $^{60}\text{Co}$  gamma calibration curve in the dose range 0-7000 rad for the EG and G Model TL-21 dosimeters.

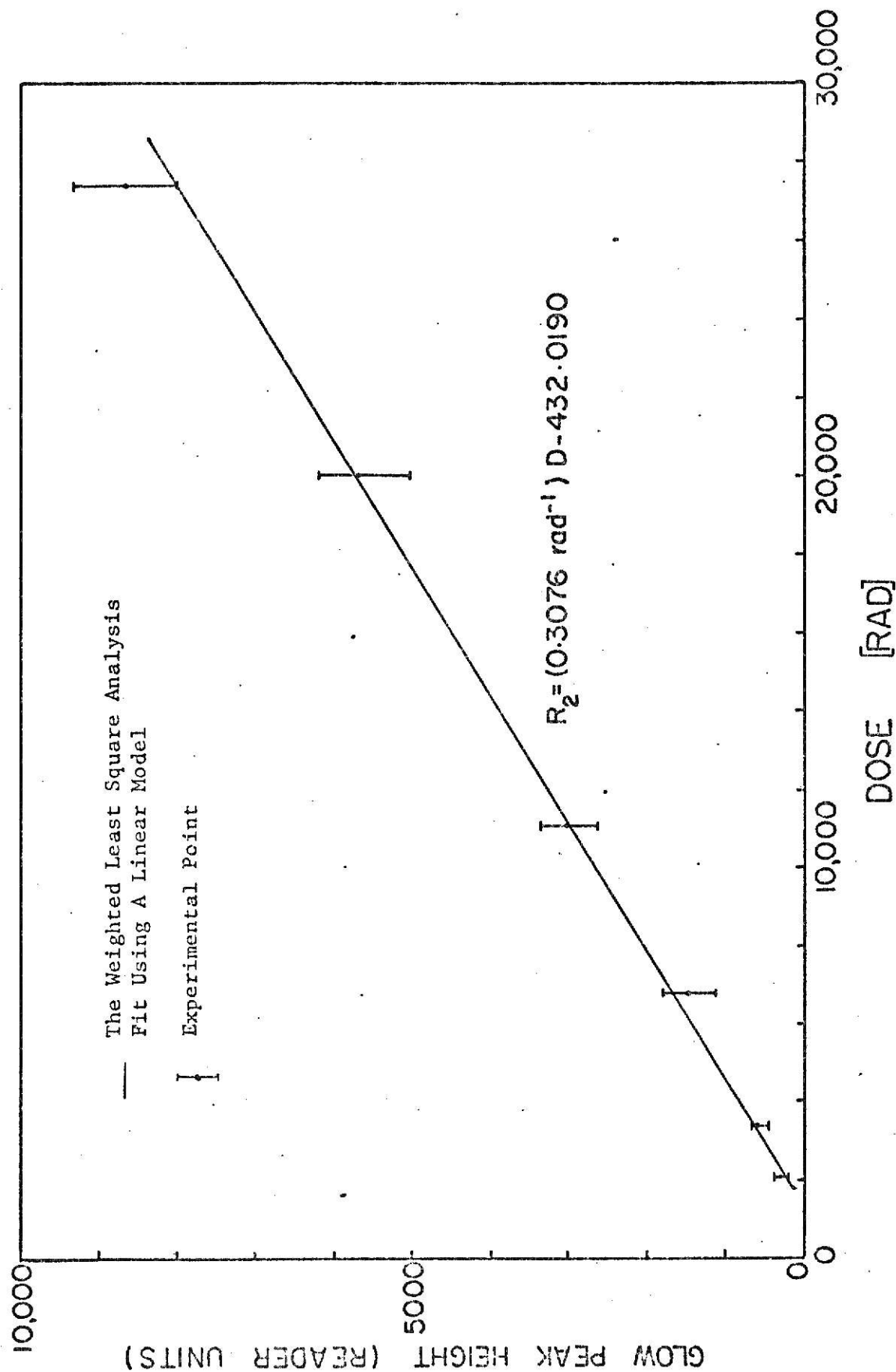


Fig. 5.2. The  $^{60}\text{Co}$  gamma calibration curve in the high dose region for the EG and G Model TL-21 dosimeters.

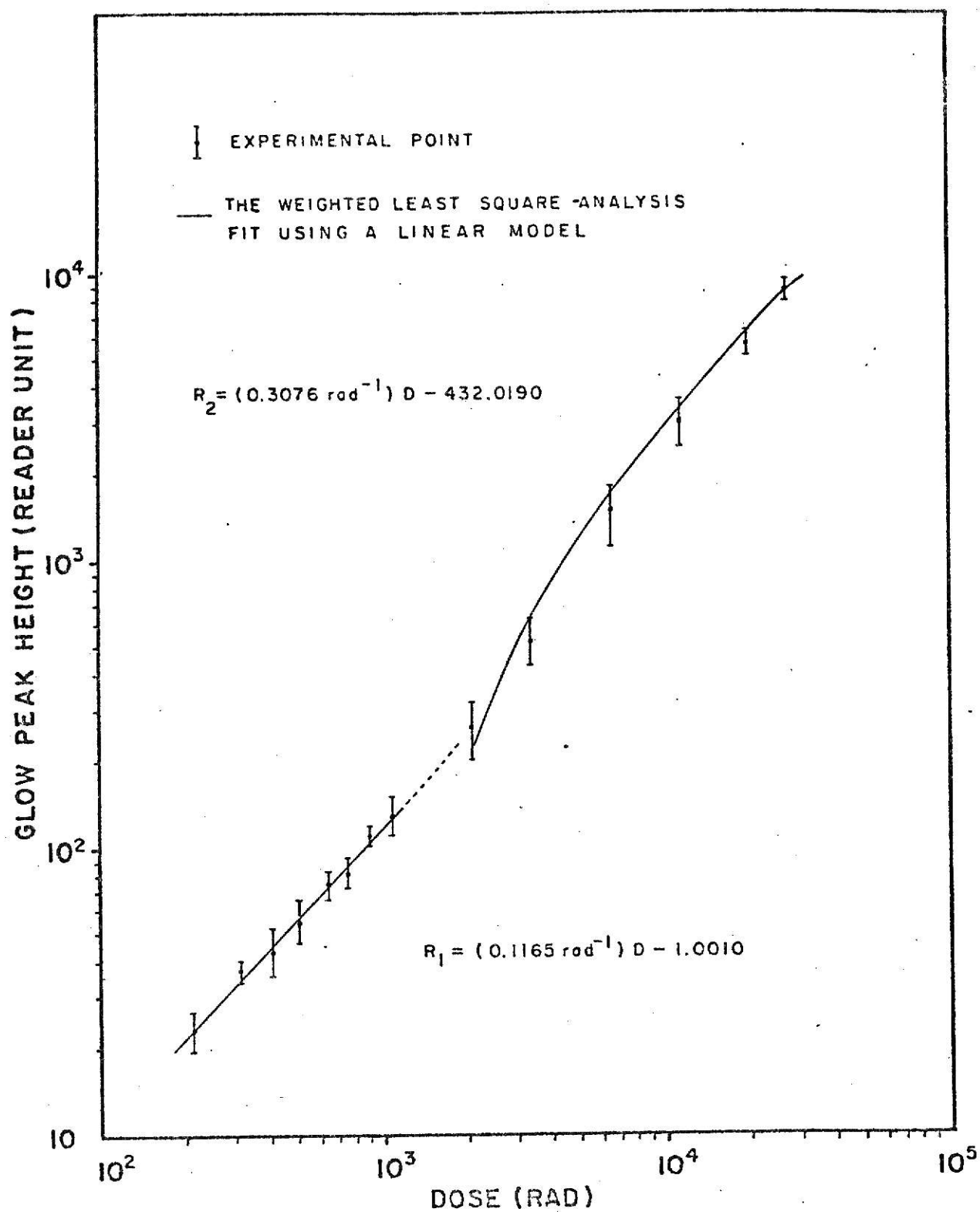


Fig. 5.3. The  $^{60}\text{Co}$  gamma calibration curve for the EG and G Model TL-21 dosimeters.

### 5.3. Neutron Calibration Curve

#### 5.3.1. General considerations.

The necessity for the neutron calibration curve arose from similar considerations as for the gamma-ray calibration curve. The exact dose rate of the  $^{252}\text{Cf}$  source was not known. Instead, integrated flux or fluence was used as a measure of dose. The fast neutron flux near the sources was determined in July 1972 by Kan (37), and the gamma dose, in the same position was determined by Kaiseruddin (38). The gamma dose is much less as compared to the neutron flux. Therefore, the  $^{252}\text{Cf}$  irradiation is referred to a neutron irradiation. The value of flux as determined by Kan (36) is also used in this study. The response  $R$  of the dosimeters in reader units was given by

$$R = \dot{R}F$$

$\dot{R}$  = calibration factor (R.U./n/cm<sup>2</sup>)

$F$  = ft. fluence n/cm<sup>2</sup>

$f$  = fast neutron flux n/cm<sup>2</sup> sec

$t$  = time of irradiation in sec.

#### 5.3.2. Experimental procedure.

The annealing procedure adopted was the same as that for gamma irradiation. The dosimeters were irradiated to dose levels ranging from a fluence of  $3.6 \times 10^{11}$  n/cm<sup>2</sup> to  $10.8 \times 10^{13}$  n/cm<sup>2</sup>. Higher dose levels were not used due to considerations mentioned earlier. The range of fluence used was such that the neutron response was of the same order of response range as the gamma response. At each experimental point, eight dosimeters were irradiated simultaneously.

### 5.3.3. Analysis of data and results.

The mean response value and the standard deviation of the response was calculated for each experimental point. The values are presented in Appendix B.

Figure 5.4 shows the calibration curve in the fluence range ( $3.5 \times 10^{11}$  n/cm<sup>2</sup> to  $75 \times 10^{11}$  n/cm<sup>2</sup>) plotted on linear scales. Here also the calibration curve is linear in both regions. However the slope of curve in the high fluence region is greater than that in the low fluence region.

Figure 5.5 is the calibration curve in the high fluence region.

Figure 5.6 is the calibration curve obtained by plotting the fluence versus the TL response on logarithmic scales.

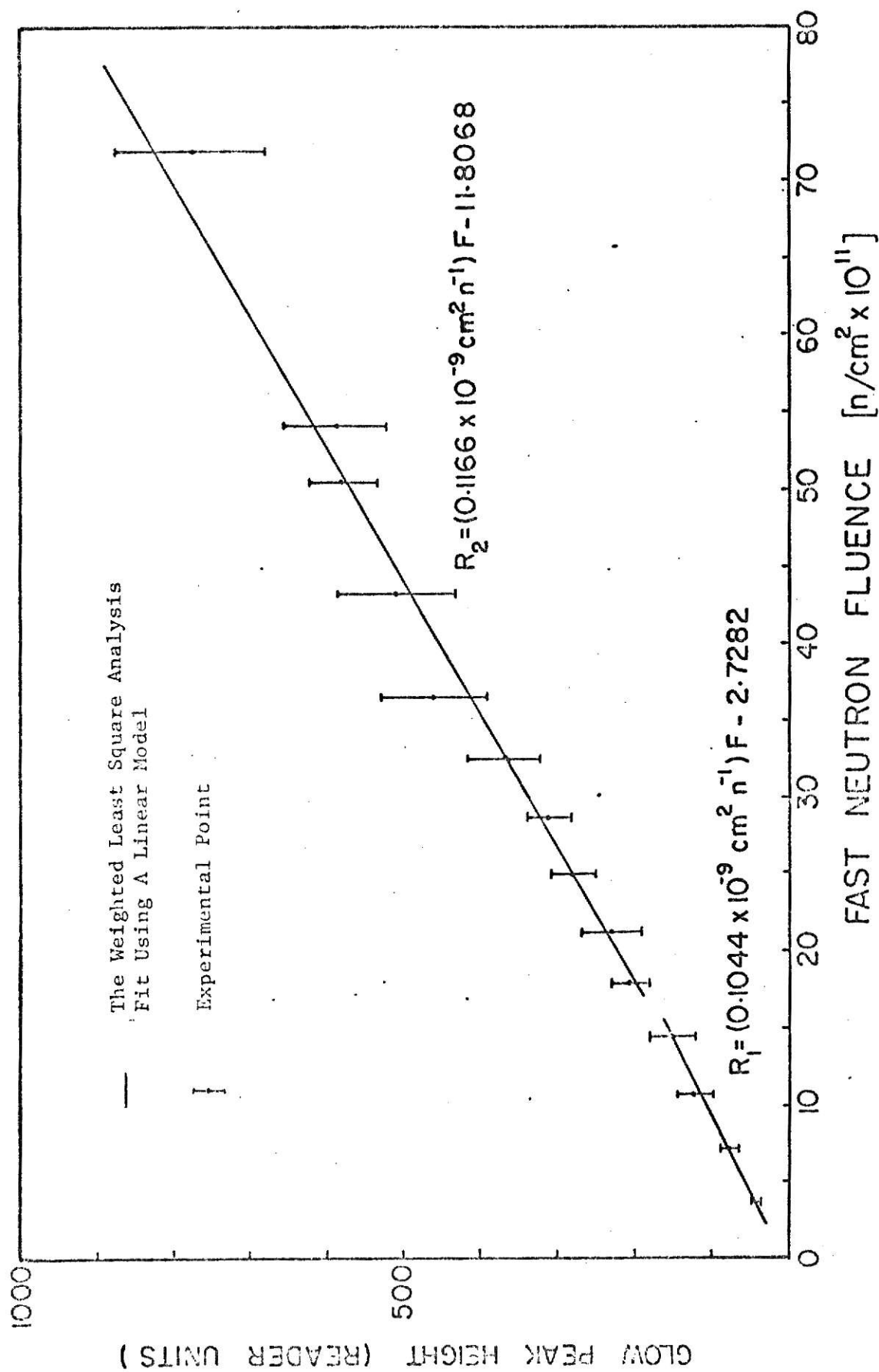


Fig. 5.4. The  $^{252}\text{Cf}$  neutron calibration curve in the fluence range 0 to  $7.5 \times 10^{11} \text{ n/cm}^2$  for the EG and G Model TL-21 dosimeter.

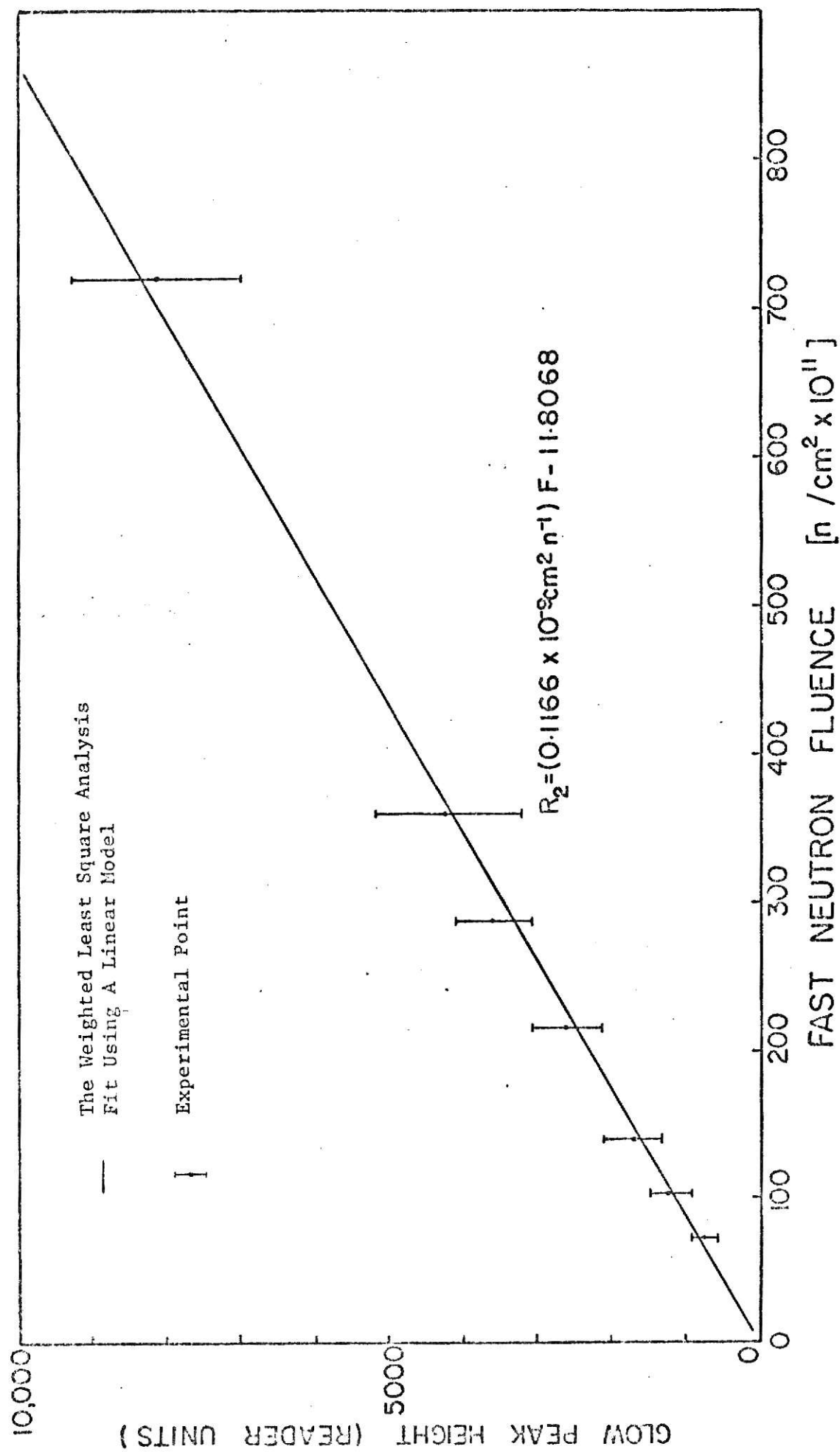


Fig. 5.5. The  $^{252}\text{Cf}$  neutron calibration curve in the high fluence region for the EG and G Model TL-21 dosimeters.

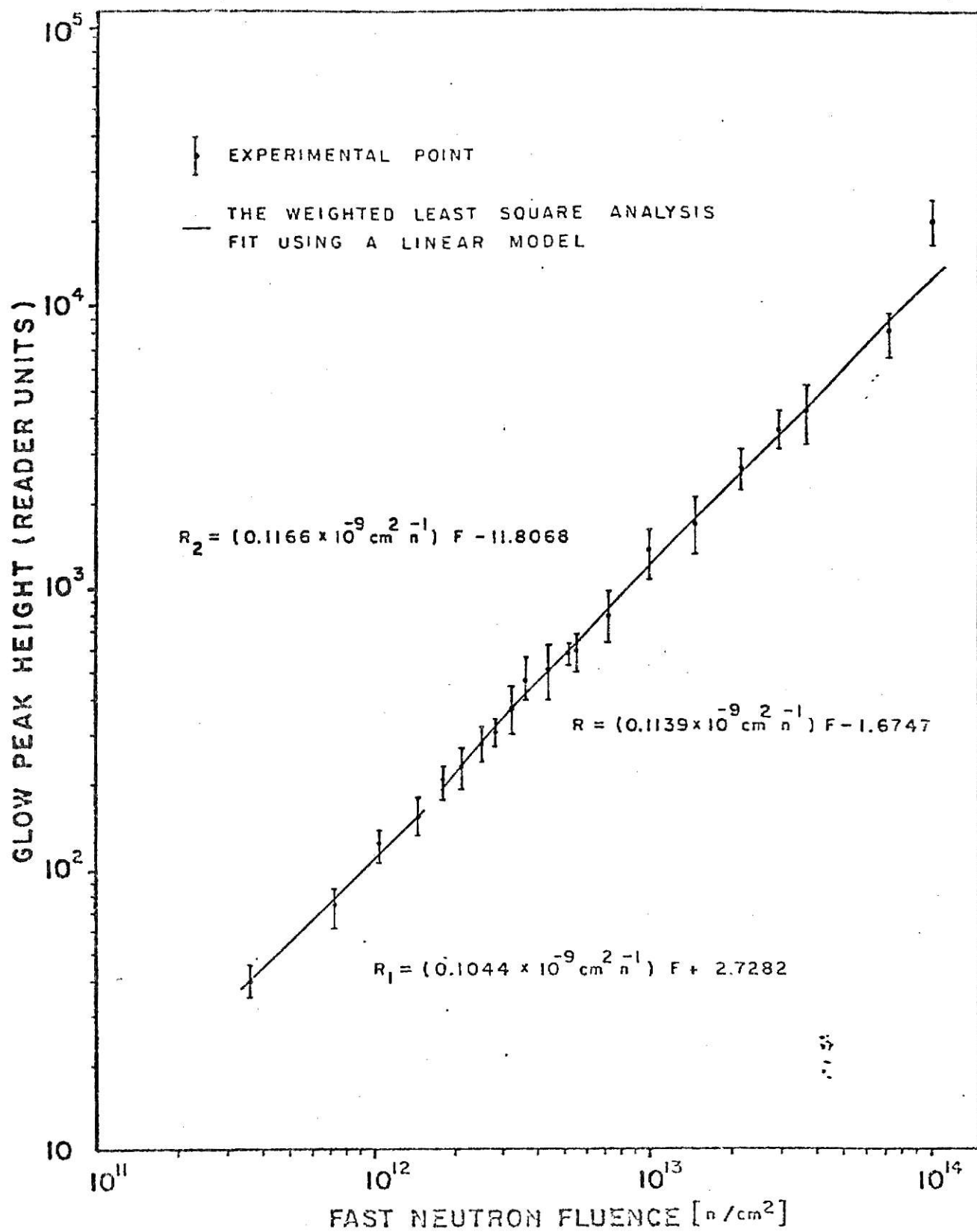


Fig. 5.6. The  $^{252}\text{Cf}$  neutron calibration curve for the EG and G Model TL-21 dosimeters.



TABLE 5.2

Parameters obtained from analysis of data for  
the neutron calibration curve.

	Slope (R.U./n cm <sup>-2</sup> )	Y-intercept (R.U.)
Low Fluence Region	$(0.1066 \pm 0.0221) \times 10^{-9}$	$2.7282 \pm 10.91$
High Fluence Region	$(0.1166 \pm 0.0077) \times 10^{-9}$	$-11.8068 \pm 27.20$

## 6. DISCUSSIONS AND CONCLUSIONS

The calibration curve for  $^{60}\text{Co}$  gamma irradiation was linear up to a dose level of  $10^3$  rad. Above that the curve exhibits supralinearity. These results agree with previous work done on LiF by several workers in this field (24,25,32,33).

The calibration curve for  $^{252}\text{Cf}$  irradiation also exhibits supralinearity above a fluence of  $1.4 \times 10^{13}$  n/cm<sup>2</sup>. The supralinearity in both curves begins in the same range of Reader Units (120 R.U. to 250 R.U.).

The presence of supralinearity in the neutron curve agrees with the results of Bliss (34), who exposed TLD-600 and TLD-700 to 14.7 MeV neutrons.

It has been reported (32,33) that the supralinearity depends upon the quality of radiation, supralinearity decreasing with increasing LET.

The exposure to the  $^{252}\text{Cf}$  source results primarily in neutron exposure as the accompanying gamma dose rate is a small fraction of the neutron dose rate (38). The fast neutron flux is much greater and the effect of thermal neutrons and gamma-rays on the response of the dosimeters may be neglected. The energy range of the neutron from the  $^{252}\text{Cf}$  source was between 2-8 MeV, the maximum number being at about 2 MeV (40). The first step in the interactions of neutrons with LiF involves the Li and F nuclei. Through different reactions such as (n,n) (n,n') (n,p) and (n, $\alpha$ ) neutrons impart their energy to Li and F ions and also produce other heavy charged particles.

TLD-100, the phosphor used in this work, is known to have 92.5%  $^7\text{Li}$  and 7.5%  $^6\text{Li}$ . There are several reactions which could be of importance for TL. The reaction with the largest cross-section above 0.1 MeV is  $^6\text{Li}(n,n)^6\text{Li}$  with a pronounced resonance at 0.255 MeV and a cross-section of 7.3 b. A

possible reaction for neutron energies above 2 MeV is the  ${}^6\text{Li}(n,dn){}_2^4\text{He}$  reaction. This has a cross-section of 0.65 b at its resonance at 5.5 MeV. Another reaction is the  ${}^6\text{Li}(n,\alpha){}_2^3\text{He}$  reaction which also exhibits a resonance at 0.255 MeV with an associated cross-section of 2.75 b. This (n, $\alpha$ ) reaction also has a thermal cross-section of about 950 b.

For  ${}^7\text{Li}$ , the dominant reaction is  ${}^7\text{Li}(n,n){}_2^7\text{Li}$  with resonances at 0.258 MeV and 5 MeV with cross-sections of 11 b and 2.07 b respectively. Above 3 MeV, the  ${}^7\text{Li}(n,tn){}_2^4\text{He}$  reaction has a maximum cross-section of about 0.4 b.

The essential difference between the gamma radiation and the neutron radiation is the large difference in their mean stopping power. From the table of LET values (33) gamma rays have a mean stopping power of about 0.52 keV/ $\mu$  whereas the 2.8 MeV alpha and the 2.8 MeV triton have a mean stopping power of 400 and 65 respectively. Thus the difference in extent of supralinearity in the response curves may be attributed to the difference in LET values of the radiation. The results support the work of Suntharlingam and others (33,32) that supralinearity is quality dependent and is an inverse function of the LET of the radiation.

The decrease in supralinearity for the neutron irradiation curve tends to indicate that no new entities are created at higher dose levels. This would then support the competing trap model as discussed in Chapter 2.

Work was done with only one kind of LiF:Mg dosimeters but the results are expected to hold for all types of LiF:Mg dosimeters.

CONCLUSIONS: The conclusions arrived at may be summarized as below:

- 1) The calibration curves for both  ${}^{60}\text{Co}$  gamma irradiation and  ${}^{252}\text{Cf}$  neutron irradiation exhibit supralinearity.

- 2) Supralinearity for both curves begins in the same range of Reader Units (120 R.U. to 250 R.U.).
- 3) The ratio of the slope of the calibration curve in the high dose region to that in the low dose region is
  - a) 2.64 for  $^{60}\text{Co}$  gamma-rays
  - b) 1.14 for  $^{252}\text{Cf}$  neutrons
- 4) Supralinearity depends upon the quality of radiation and is an inverse function of the linear energy transfer (LET) of the radiation.

## 7. ACKNOWLEDGEMENTS

The author wishes to express her gratitude to Dr. Joseph F. Merklin and Dr. Hermann J. Donnert for their continuous guidance and help. Thanks are due to the faculty and staff of the Nuclear Engineering Department for their friendly and cooperative attitude.

The financial support from the Office of Naval Research is gratefully acknowledged.

The author is also indebted to her parents for their encouragement and help in making the stay in this country possible.

## 8. LITERATURE CITED

1. E. P. Blizzard, "Reactor Handbook," Interscience Publishers, New York, New York, 1962.
2. M. A. Northup and O. I. Lee, J. Opt. Soc. Am. 30, 206 (1940).
3. F. Daniels, C. A. Boyd and D. F. Saunders, Science 117, 343 (1953).
4. J. R. Cameron, D. W. Zimmerman, G. W. Kenney, et al, Health Phys. 10, 25 (1964).
5. F. H. Attix, NRL Report 6145 (1964).
6. R. J. Ginther and R. D. Kirk, J. Electrochem. Soc. 271, 253 (1963).
7. B. Bjärngard, Luminescence Dosimetry, USAEC Rept., CONF-650637, 195 (1965).
8. J. H. Schulman, et. al., Luminescence Dosimetry, USAEC Rept., CONF-650637, 113, (1965).
9. J. H. Schulman, Luminescence Dosimetry, USAEC Rept., CONF-650637, 7 (1965).
10. Z. Spurny, At. En. Rev. 3, No. 2, 61 (1965).
11. C. Distenfeld, W. Bishop and D. Colvett, Luminescence Dosimetry, USAEC Rept., CONF-650637, 457 (1965).
12. G. W. R. Endres, Luminescence Dosimetry, USAEC Rept., CONF-650637 435 (1965).
13. C. L. Wingate, E. Tochilin and N. Goldstein, Luminescence Dosimetry, USAEC Rept., CONF-650637, 421 (1967).
14. P. S. Weng, IEEE Transactions, Nucl. Sci., 13, 222 (1966).
15. C. A. Coulson, "Valence", 2nd Ed., Oxford University Press, New York and London (1961).
16. C. Kittel, "Introduction to Solid State Physics," John Wiley and Sons, Inc., New York (1967).
17. J. G. Calvert and J. N. Pitts, Jr., "Photochemistry," John Wiley and Sons, Inc., New York (1966).
18. J. H. Schulman, R. J. Ginther, et al., Nucleonics 18, 92 (1960).
19. J. R. Cameron, D. W. Zimmerman and R. W. Bland, Luminescence Dosimetry, USAEC Rept., CONF-650637, 47 (1965).

20. J. T. Randalls and M. H. F. Wilkins, Proc. Roy. Soc. (London) A184, 365 (1945).
21. G. F. J. Garlick and M. H. F. Wilkins, Proc. Roy. Soc. (London) A184, 408 (1945).
22. D. W. Zimmerman, C. R. Rhyner and J. R. Cameron, Health Phys. 12, 525 (1966).
23. J. R. Cameron, N. Suntharlingam and C. R. Wilson, CONF-680920, USAEC Dept., 332 (1968).
24. E. N. Claffy, C. C. Klick and F. H. Attix, CONF-680920, USAEC Rept., 302 (1968).
25. M. Kaiseruddin, M.S. Thesis, Kansas State University (1968).
26. C. J. Karzmark, J. F. Fowler and J. T. White, Int. J. App. Rad. Isotopes, 17, 161 (1966).
27. N. P. Dean and J. H. Larkins, USAEC Rept., LAMS-3034, 205 (1963).
28. C. R. Wilson, L. A. DeWerd and J. R. Cameron, USAEC Rept., COO-1105-116.
29. L. A. DeWerd and J. R. Cameron, USAEC Rept., COO-1105-118.
30. F. F. Morhead and F. Daniels, J. Chem. Phys., 27, 1318 (1957).
31. Y. P. Naylor, Phy. Med. Biol. 10, 564 (1965).
32. J. Wagner and J. R. Cameron, USAEC Rept., COO-1105-117.
33. N. Suntharlingam, USAEC Rept., COO-1105-129.
34. C. Bliss, M.S. Thesis, Kansas State University, 1967.
35. J. Kastner, B. G. Oltman and P. Tedeschi, Health Phys. 12, 1125 (1966).
36. "TL Dosimetry System, Models TL-3B and TL-3C," Operation Manual #S-316-MN, EG and G, Santa Barbara Division (1966).
37. C. G. Kan, M.S. Thesis, Kansas State University, (1973).
38. M. Kaiseruddin, Ph.D. Dissertation, Kansas State University, (1973).
39. G. W. Snedecor, "Statistical Methods," The Iowa State University Press, Ames, Iowa.
40. D. Prigel, M.S. Thesis, Kansas State University (1972).

41. J. R. Cameron, et al., "Thermoluminescent Dosimetry," The University of Wisconsin Press, Madison, Milwaukee (1968).
42. S. K. Mehta, Ph.D. Dissertation, Kansas State University (1972).
43. K. Ayyanger, A. R. Reddy and C. L. Brownell, USAEC Rept., CONF-680920 525 (1968).



## 9. APPENDICES

## APPENDIX A

## Data and Results for the Gamma Radiation Calibration Curve

Sample Number	Duration of irradiation (sec)	Timed Dose	Total Dose	Response (reader units R.U.)
1	3	99.75	216.55	23.87 $\pm$ 4.02
2	6	199.5	316.3	37.24 $\pm$ 3.99
3	9	299.25	416.05	43.87 $\pm$ 9.24
4	12	399.0	515.8	54.69 $\pm$ 12.09
5	15	532.0	648.8	74.62 $\pm$ 8.9
6	20	639.99	765.79	80.66 $\pm$ 13.38
7	25	799.99	916.80	110.83 $\pm$ 11.14
8	30	997.5	1113.75	127.87 $\pm$ 26.32
9	60	1995.0	2111.8	262.88 $\pm$ 69.44
10	100	3325.0	3441.8	523.13 $\pm$ 110.68
11	200	6649.9	6766.8	1467.5 $\pm$ 448.39
12	350	11637.5	11754.3	3007.5 $\pm$ 434.08
13	600	19950.0	20066.8	5662.5 $\pm$ 678.1
14	820	27264.9	27381.8	8785.7 $\pm$ 853.28

Dose rate in Gammacell = 33.25 rad/sec

## Data and Results for the Neutron Radiation Calibration Curve

S. No.	Duration of Irradiation (min)	Fluence (n/cm <sup>2</sup> ) x 10 <sup>11</sup>	Response (Reader Units)	
1	1	3.6	40.45 ±	5.37
2	2	7.2	74.31 ±	18.85
3	3	10.8	121.25 ±	27.90
4	4	14.4	151.70 ±	30.52
5	5	18.0	204.90 ±	30.09
6	6	21.6	229.25 ±	39.87
7	7	25.2	281.29 ±	39.54
8	8	28.8	312.0 ±	34.08
9	9	32.4	368.50 ±	81.73
10	10	36.0	463.60 ±	108.28
11	12	43.2	510.00 ±	135.00
12	14	50.4	581.40 ±	45.15
13	15	54.0	584.87 ±	126.12
14	20	72.0	778.57 ±	200.60
15	30	108.0	1373.75 ±	322.70
16	40	144.0	1706.60 ±	453.15
17	60	216.0	2637.50 ±	494.30
18	80	288.0	3656.63 ±	535.77
19	100	360.0	4267.10 ±	1121.10
20	200	720.0	8144.28 ±	1634.30
21	300	1080.0	11385.7 ±	1647.65

Value of flux taken as  $6.0 \times 10^9$  n/cm<sup>2</sup> sec.

THERMOLUMINESCENT RESPONSE OF LiF:Mg TO  
GAMMA AND NEUTRON RADIATION

by

NALINI KHANNA

M.Sc., Indian Institute of Technology, N. Delhi, INDIA, 1970

---

AN ABSTRACT OF A MASTER'S THESIS

submitted in partial fulfillment of the  
requirements for the degree

MASTER OF SCIENCE

Department of Nuclear Engineering

KANSAS STATE UNIVERSITY  
Manhattan, Kansas

1973

## ABSTRACT

Theory of thermoluminescence and thermoluminescent dosimetry was reviewed. The competing trap model for supralinearity was discussed. Factors affecting the thermoluminescence of LiF:Mg were briefly reviewed.

Calibration curves for  $^{60}\text{Co}$  gamma radiation in the dose range  $2 \times 10^2$  rad to  $3 \times 10^5$  rad, and for  $^{252}\text{Cf}$  neutron radiation in the fluence range  $3.6 \times 10^{11}$  n/cm<sup>2</sup> to  $1.08 \times 10^{14}$  n/cm<sup>2</sup> were obtained.

The nature of the calibration curves was investigated. Presence of supralinearity was determined by dividing the curves in two regions, the low dose region and the high dose region. In each region the data were fitted to a linear model using a weighted least square analysis fit.

The conclusions drawn from analysis of the data were:

1. The calibration curve for  $^{60}\text{Co}$  gamma irradiation exhibits supralinearity above a dose of  $10^3$  rad. The slope of the curve in the nonlinear region is 2.6 times that in the linear region.
2. The calibration curve for  $^{252}\text{Cf}$  neutron irradiation also exhibits supralinearity above a fluence of  $14.4 \times 10^{11}$  n/cm<sup>2</sup>. The ratio of the slope in the nonlinear region to that in the linear region is 1.12.
3. Evidence of supralinearity for both types of radiation begins in the same range of Reader Units (120 R.U. to 250 R.U.).
4. Supralinearity depends on the quality of the radiation, being inversely proportional to the LET of the radiation.